

Capillary optical fiber – design, fabrication, characterization and application

R. ROMANIUK*

Institute of Electronic Systems, Warsaw University of Technology,
15/19 Nowowiejska St., 00-665 Warsaw, Poland

Abstract. The paper presents a modification of capillary optical fibers fabrication method from an assembled glass preform. A change of dimensional proportions in the capillary optical fiber drawn from a single preform is allowed on-line via the control of overpressure and thermal conditions in the outflow meniscus which essentially lowers the manufacturing costs. These conditions are among the solutions (velocity fields) of the Navier-Stokes equations adapted to the capillary optical fiber pulling geometry and temperature distribution in the oven. The velocity fields give solutions to other quantities of interest such as flow rate, pulling force and fiber geometry. The calculation and experimental results for capillary optical fibers were shown in the following dimensional range: internal diameters 2–200 μm , external diameters 30–350 μm , within the assumed dimensional stability (including ellipticity) better than 1%. The parameters of fabricated capillary optical fibers of high-quality low-loss optical multicomponent glasses were: losses; 100 dB/km, mechanical strength above 1GPa with Weibull coefficient in the range 3–7, internal numerical aperture 0.1–0.3, external numerical aperture 0.1–0.3, core index 1.5–1.8, transparency 0.4–2 μm , thermally and/or chemically conditioned internal surface, double polyimide protection layer, soft or hard jacketed, connectorized. The capillary optical fibers were applied in our own and several external laboratories in spectroscopy, refractometry, micro-fluidics and functional microoptic components. The paper summarizes a design, technological and application work on capillary optical fibers performed during a recent national research program devoted to optoelectronic components and modules.

Key words: capillary optical fibers, optical fiber technology, hollow core optical fibers, optoelectronics

1. Introduction

A capillary optical fiber (COF) consists of an annular, ring-like, doughnut-shaped, high-index optical core around an air hole, a low-index optical cladding and a protective, high-index polymer jacket (coating). Optical wave propagation in a capillary depends essentially on the geometrical distribution of empty areas in the cross section of the fiber and refractive index distribution near glass-air boundary. Refractive structure of the cladding is uniform or has an index depression around the core. Capillary optical fibers are low-loss optical glass [1], or amorphous polymer, multilayer filaments in which uniquely the wave [2] and matter [3] can be simultaneously propagated likewise and counter wise. The axial hole in a COF is perfectly circular, quasi-circular (multiangular) or with periodic, angularly distributed surface artifacts, in a photonic COF – for removal of surface modes, elliptical, square or complex. The axial hole in COF is longitudinally uniform, linearly or exponentially tapered for fiber to fiber coupling, optical power focusing, mode conversion, periodically or aperiodically wrinkled for modal radiation characteristics design between fiber layers.

The empty core is evacuated or filled with an active medium as vapor, water, gas – like hydrogen or methane [4], liquid [5], liquid crystal, self-assembling colloidal crystal or stream of single, cold, optically guided rather than ballistic particles – like atoms, molecules or nanocrystallites. The aim of filling the hollow core is to confine the interaction between

the wave and matter to a minute area in the cross section but of considerable optical length in the capillary. The interaction processes get amplified many orders of magnitude by big optical gradients (not necessarily by the intensity alone) and the path.

The internal surface of COF is pure pristine glass – left isolated in vacuum from the very moment of fiber manufacturing, conditioned glass – either silanized, hydrated, processed for passivation of unbound oxygen bridges, or lined with a variety of immobilized activating thin-film layers including electrostatically self-aligning layers of high adhesion [6]. The aim of conditioning or lining of the internal capillary surface is to prepare it to the role of a reaction base, immobilizing matrix or catalyst between different interacting streams of matter and wave. After the reaction and optical measurement, the lining layer is to be developed, polymerized, chemically or optically modified, partially or completely washed out, to prepare the inner surface of COF for the same, changed or a different process.

Propagation characteristics of the COF, including single-mode or multimode, guided or weakly-leaking modes, depend on the state of internal surface of the fiber, relative dimensions of the hollow core to the wavelength and refractive/diffractive structure of glass, and other dielectric – like polyolefines, semiconductor – like germanium, or noble metal layers [7] encircling the core. A large difference of indexes on the internal air-glass boundary in the optical core of COF causes

*e-mail: elka.pw.edu.pl

that the fundamental mode LP_{01} (contrary to a classical, step-index singlemode optical fiber) may have a finite value of the cut-off frequency. Cut-off of the fundamental mode in COF (similarly to W-profile and M-profile optical fibers) depends on the fiber construction. The condition for a fundamental mode to possess a nonzero cut-off frequency in a singlemode COF is that the average value of the refraction in the core area (embracing optical core and a hole) has to be lower than the average refraction in the cladding. The area of this property is called a negative dielectric volume [8]. Existence of a nonzero cut-off for the fundamental mode makes from such a COF a tunable distributed modal filter. The filter is fabricated in practice of a tapered length of a fiber. When the COF core is elliptical or distorted cylindrical, the fiber displays birefringence and polarization maintaining capability.

The fundamental, singlemode, ring-like, dark hollow beam of light (DHB) of zero intensity on the axis, propagating in the COF has broad applications in atom optics, microoptics and telecommunications. Field gradient inside the beam exerts a repulsive potential for particles, keeping them on the fiber axis. The fundamental mode of ring-like field distribution may be nearly lossless converted to a Gaussian beam in a tapered mode converter and then coupled to a spliced length of a classical singlemode optical fiber. It is a basic advantage of the singlemode COF. A low-order multimode COF is used for excitation of higher order modes in a classical multimode optical fiber for multimode dispersion compensation in gigabit Ethernet systems, and as a spectrally tuned waveguide filter. A ring-like optical core facilitates coupling of large optical power into the COF because of a larger value of the core to cladding area ratio, in comparison with a classical singlemode step-index optical fiber. A singlemode COF fulfills the following conditions: has a large core in which the fundamental LP_{01} mode is propagated, without the presence of the next LP_{02} mode, the fundamental mode has a nonzero and practically realizable value of the cut-off frequency, there are conditions to suppress the unwanted emission, including the stimulated Raman scattering (SRS) in a certain wavelength range, and transmission of this radiation along the COF.

Fabrication techniques of discrete COF differ for pure or high silica glasses and soft glasses and include: MCVD preform with incomplete collapsing, hollow core preform or pressurized multi-crucible [9]. The capillaries, 10–200 mm in length, are also manufactured during VLSI – like process and remain embedded in a silicon substrate as a product of local oxidation or LPVCD.

The COFs are also referred to as hollow core optical fibers. The name of holey optical fibers is also used. The variety of names stems from a construction and technology mixture of discrete capillary optical fiber and photonic crystal fiber with a large hollow core and a network of small holes. Thus, an additional description is needed for a fiber to distinguish its construction in a particular case. Hollow core optical fibers (HCF) mean frequently photonic bandgap (or PBG) fibers, where the light guidance in low index region is provided by periodic dielectric structures (photonic crystals). Alternatively, for a capillary optical fiber a structure is usually meant

with no PBG but with an annular optical core of high, step or gradient, index surrounded by a homogeneous or depressed index optical cladding.

Applications of COF stem from either well established chemical capillaries or newer technologies which include: miniaturization, integration, adaptation to planar topology, micromachining, optical measurements, matter and wave co-propagation, multifunction capabilities, intelligence, redundancy and reliability, etc. The application fields of COF and integrated capillaries may be generally divided to the following areas:

- classical chemical capillary column technologies, like electrophoresis and chromatography,
- new complex and miniaturized chemical capillary technologies including merging of chemical reactants, derivatization and labelling, micro- and nanoliter reactions, microfluidics, pattern determination in picoliter bubble-train flows, lab-on-capillary systems,
- optically enhanced chemical capillary technologies, like evanescent wave absorbance, optical and ultrasonic spectroscopy and spectrofluorometry,
- typical fiber optic areas like low power, trunk and high power optical transmission in a hollow core, liquid core fibers, aligning components like ferrules, and connectors, optical microcomponents, microstructures, mode converters, specialized signal transmission and processing,
- liquid light guides of large dimensions and large NA for UV, visible and IR illumination,
- high power visible and IR transmission with optical capillaries of complex multilayered construction for FEL lasers, with metal inserts covered with dielectrics [10], made from oxide glasses, and chalcogenide glasses or bundled COFs,
- high power COF guides for CO_2 laser and for UV laser,
- hollow core photonic crystal fibers with guidance based on photonic bandgap (PBG),
- capillary optics for X-ray transmission [11],
- atom optics, deBroglie wave transmission by optical potential well of the dark hollow beam (DHB) in COF for controlled atomic guidance and deposition,
- optical fiber nanocapillaries,
- lab on a chip systems referred to as chemical microsystems or chemical MOEMS, which are evolving to very complex, hybrid integrated circuits,
- COF lasers [12],
- hollow core photonic crystal fibers with guidance related to Von Neumann-Wigner bound and quasi-bound states within a continuum.

The current research on COF based sensors and photonic functional devices concentrates on: multichannel optical capillary systems, evanescent wave measurements, ion optodes of heavy metals – like chromium, absorbance spectroscopy, sub-microliter spectrometry, high-pressure Raman spectroscopy, optical-fiber based multi-wavelength electrophoresis, refractometry [13], viscometry, microfluidics [14] with semiconductor deposited inside a COF, gas sensing, biosensing, medical, chemical sensing [15], fluorimetry with liquid crystal core

capillaries, temperature sensor with Bragg grating capillary, laser trapping of crystallites in hollow optical fibers, atom optics, mode converters and filtering for telecommunications, stimulated Raman scattering suppressors, hollow fiber lasers, and many others.

The research on COF and their applications is also active in this country. Two major areas are photonic crystal based (PCF) holey optical fibers, manufactured in Lublin [16] and hollow core (non PCF) optical fibers manufactured in Białystok [17]. A recent national program on optoelectronic components and modules PBZ-MIN-009/T11/2003 [18], coordinated by CTT Warsaw University of Technology and ITME Warsaw, triggered an interest among many laboratories in research and practical applications of available technological variety of COFs. Some of these applications include: high mechanical strengths COFs, nanoliter microdroplet manipulation in an optical capillary [19], refractometry [20], thermometry [21], integrated capillary microcomponents, telecommunications, high power transmission, modeling of matter and wave co-propagation, rare-earth doping of capillaries and annular core optical fibers, liquid crystal core fibers, a number of other sensors and functional devices.

2. Design

It is justified to take an assumption of weak guidance of linearly polarized modes in a COF, similarly to classical optical fibers. This approximation assumes propagation of LP modes instead of HE and EH hybrid modes (with longitudinal field components) supplemented with fully transverse TEM modes. The validity of this assumption was proved for a whole class of refractive profiles including W, M and hollow core fibers [2, 8]. A necessary and sufficient condition for the weak guidance to be right is a small difference of refraction in the fiber cross-section. If so, the only doubt is associated with a large refraction difference between the air and glass part of the COF core. The whole area of low-refraction capillary hole and high refraction adjacent glass is seen by the fundamental mode of such a structure LP_{01} as an optical core. This large, intra-core, differential refraction does not undermine the assumption for weak guidance in a singlemode COF for small dimensions of the capillary and optical layers. Guidance characteristics of the fundamental mode are influenced not only by the absolute differential refraction but also by the average physical refraction of the core and cladding.

The input data for refraction and geometry in a COF for the modal analysis are:

- refractions: capillary $n_o = 1$, n_r core, n_p cladding, n_d depressed cladding,
- differential refractions: Δn_{rd} , Δn_{rp} , Δn_{pd} , numerical aperture: $NA_r = \sqrt{n_r^2 - n_p^2}$, $NA_d = \sqrt{n_p^2 - n_d^2}$,
- radiuses of areas: r_c capillary, r_r core, r_d refractive depression in cladding,

- thickness of areas: $d_c = 2r_c$, $d_r = r_r - r_c$ core, $d_d = r_d - r_r$ refractive depression in cladding,
- refraction for analyzed COFs: high silica $n_p = 1.46$, compound glass $n_p = 1.56$, for $\lambda = 1\mu\text{m}$.
- numerical aperture: $NA = 0.1$ for high silica fibers and $NA = 0.2$ for compound glass fibers.
- dimensions: $r_c = 1 - 10\mu\text{m}$ for all fibers.

A fiber with a uniform cladding is called a COF, while a fiber with non-uniform cladding is called a DCCOF (depressed cladding COF).

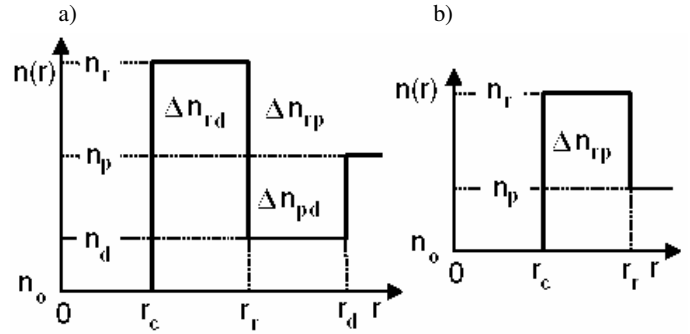


Fig. 1. Refraction and geometric data for a) DCCOF and b) COF

The electrical field component of a weakly guiding mode has a form: $E(r, \phi, z) = e(r) \exp(-jm\phi) \exp(-j\beta z)$, where r , ϕ – radial and angular coordinates in a plane perpendicular to the fiber axis, z – length measured along fiber axis, $m = 0, \pm 1, \pm 2, \dots$ – azimuthal mode number, β – propagation constant of a mode associated with effective refraction via the relation $n_{eff} = \beta/k_o$, $k_o = 2\pi/\lambda$ is a wavenumber in vacuum. Radial dependence of transverse field component $e(r)$ is an eigensolution of Helmholtz equation of the form: $e(r) = A_0 I_m(vr)$ for $r < r_c$; $A_1 J_m(ur) + A_2 Y_m(ur)$ for $r_c < r < r_r$; $A_3 K_m(wr)$ for $r > r_r$, in a COF, and $e(r) = A_0 I_m(vr)$ for $r < r_c$, in a DCCOF. $A_1 J_m(ur) + A_2 Y_m(ur)$ for $r_c < r < r_r$; $A_3 I_m(wr) + A_4 Y_m(wr)$ for $r_r < r < r_d$; $A_5 K_m(sr)$ for $r > r_d$, where $A_i (i = 0, 1, 2, 3, 4, 5) = \text{const}$. J_m , Y_m are Bessel functions of the first and second kind, I_m , K_m are modified Bessel functions of the first and second kind, m – th order. Modal parameters, which are Bessel function arguments v , u , w , s for particular refraction areas of fiber cross section with periodic and aperiodic field distribution, are defined: $v^2 = \beta^2 - k_o^2$, $u^2 = n_r^2 k_o^2 - \beta^2$, $w^2 = \beta^2 - n_p^2 k_o^2$, $s^2 = \beta^2 - n_d^2 k_o^2$. Field values and fields derivatives in the radial direction must be continuous on every boundary in the fiber cross-section: $e(r_c^-) = e(r_c^+)$, $de(r_c^-)/dr = de(r_c^+)/dr$, $e(r_r^-) = e(r_r^+)$, $de(r_r^-)/dr = de(r_r^+)/dr$, $e(r_d^-) = e(r_d)$, $de(r_d^-)/dr = de(r_d)/dr$. A characteristic equation is formed from these conditions. The following matrices have to assume zero value, for COF, where the apostrophe means Bessel function derivative:

$$\begin{vmatrix} I_m(vr_c) & -J_m(ur_c) & -Y_m(ur_c) & 0 \\ vI'_m(vr_c) & -uJ'_m(ur_c) & -uY'_m(ur_c) & 0 \\ 0 & J_m(ur_r) & Y_m(ur_r) & -K_m(wr_r) \\ 0 & uJ'_m(ur_r) & uY'_m(ur_r) & -wK'_m(wr_r) \end{vmatrix} = 0 \quad (1)$$

and analogically for DCCOF:

$$\begin{vmatrix}
 I_m(vr_c) & -J_m(ur_c) & -Y_m(ur_c) \\
 vI'_m(vr_c) & -uJ'_m(ur_c) & -uY'_m(ur_c) \\
 0 & J_m(ur_r) & Y_m(ur_r) \\
 0 & -uJ'_m(ur_r) & -uY'_m(ur_r) \\
 0 & 0 & 0 \\
 0 & 0 & 0 \\
 0 & 0 & 0 \\
 0 & 0 & 0 \\
 -I_m(wr_r) & -K_m(wr_r) & 0 \\
 -wK'_m(wr_r) & -K'_m(wr_d) & 0 \\
 I_m(wr_d) & K_m(wr_d) & -K_m(sr_d) \\
 wI'_m(wr_d) & wK'_m(wr_d) & -sK'_m(sr_d)
 \end{vmatrix} = 0. \tag{2}$$

The propagation constant β_{ml} and wave parameters v, u, w, s are obtained by numerical solution of the characteristic equation for each azimuthal m and radial $l = 1, 2, 3, \dots$ mode number. The modal cut-off is when the effective refraction is equal to cladding refraction. The transverse field distribution is obtained from equations $e(r)$ after determination of A_i constants from the β_{ml} . Figures 2–5 present calculation results for COF and DCCOF fibers of given parameters.

Below, there are gathered some conclusions from the numerical solutions, related to the applications of COF. Basic differences between a classical, step-index, singlemode optical fiber and a COF were emphasized. The following properties of all fiber modes are completely determined by the effective refraction: field distribution, dispersion, overlap integral of modal field with the core, micro-bending losses, mode susceptibility to refraction and geometry changes in the fiber. The effective refraction may change within the boundaries determined by maximal and minimal physical refractions in the fiber. The rate of change for effective refraction and mutual distances between its quantized values are determined by local averaged value of physical refraction (refractive profile).

The reverse, squared refractive profile plays a role of a potential well. Comparison of a full vectorial analysis, done in MatLab environment, with the LP approximation yields an error not bigger than a fraction of %, for the most practical constructions of COF, further supporting the validity of weak guidance assumption.

The fundamental mode in both cases is LP_{01} . The fundamental mode in a COF has zero field value at the fiber axis, while in a classical fiber it reaches the maximum. A single-mode classical optical fiber of step-index and simple monotonic gradient profiles has always a zero value of the cut-off frequency for the fundamental mode. A COF (as well as M and W fibers) has a nonzero cut-off frequency of the fundamental mode then, and only then, when the averaged value of the whole optical core refraction is lower than the relevant refraction in the cladding. A local depression of refraction in the cladding, height of refraction in the core and change in geometrical proportions of these areas lead, when the non-zero cut-off does exist, to the effective change of the cut-off value, what was presented in Fig. 2. Changes in the cut-off of fundamental mode turns the COF to an effective modal converter and filter, with the efficiency measured by the rate of the cut-off sweep against the normalized frequency V . The modal field selectivity is determined by the value of dn_{eff}/dV in the vicinity of cut-off.

An annular distribution of field in the fundamental mode facilitates pumping the COF with optical power nearly an order of magnitude higher than in a classical step-index singlemode optical fiber. Singlemode and multimode COFs are extensively used in optical fiber lasers as an active medium and for a number of functional devices.

A small diameter of the hole causes larger separation between the fundamental mode and the next one. Simultaneously, the fundamental mode enters deeper into the optical cladding. The cut-off wavelength of LP_{01} increases with the hole diameter. The changes in cut-off for fundamental mode with the hole diameter are small in comparison with the relevant changes for higher order modes. The cut-off of a fun-

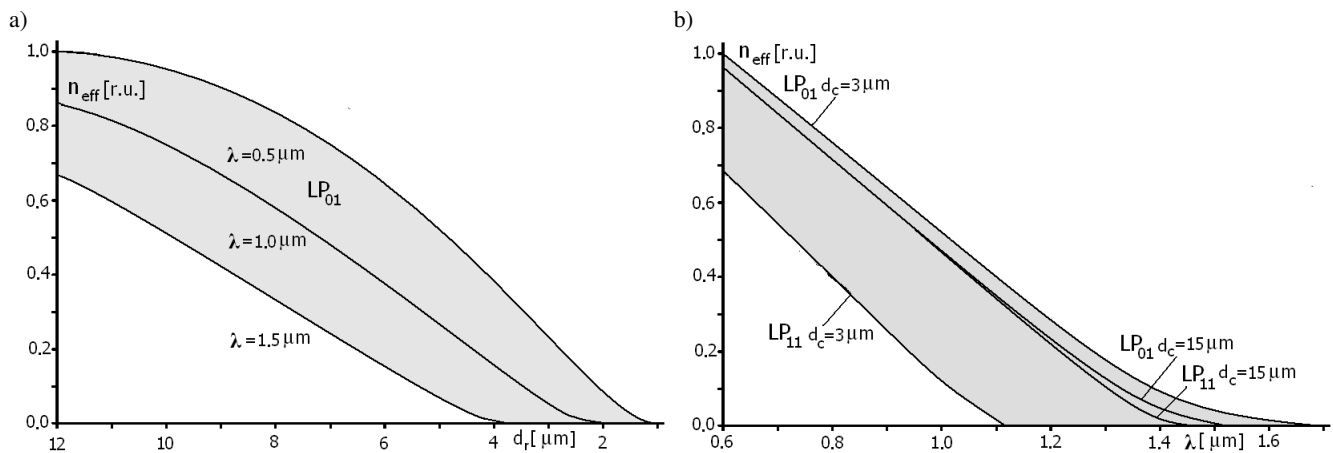


Fig. 2. Calculated relative, effective refraction of the fundamental mode in a COF made of high silica glass: (a) as a function of optical core thickness for different wavelengths, for $d_c = 5 \mu\text{m}$, (b) as a function of wavelength for different capillary diameters, for $d_r = 5 \mu\text{m}$, [r.u.] – relative units

damental mode is relatively soft and slow. The values of derivatives dn_{eff}/dd_r and $dn_{eff}/d\lambda$, for $n_{eff} \approx n_p$ are small, which determines weak properties of such a fiber as a modal filter. When the fundamental mode is far from cut-off, or equivalently is strongly guided, the value of effective refraction is relatively high and sensitivity of the mode to fiber geometry (including microbending) and refraction is low. Such a fiber is not a source of modal noise. Coiling the COF (similarly to W and M fibers) causes shortening cut-off of the fundamental mode.

A large diameter of the hole (of the order 10λ), what was presented in Fig. 2b causes nearly total overlapping of the cut-off characteristics for the fundamental mode and the next one. This means that the COF of large hole, even for thin core of high refraction (which acts contradictory) is susceptible to carrying many modes and the separation of these modes from the fundamental one turns impossible. However, separation of the modes LP_{02}, LP_{03}, \dots from the fundamental one in a low mode COF is possible, while the separation of modes P_{11}, LP_{21}, \dots is nearly impossible. In a multimode COF

of large dimensions of the refractive areas in comparison with the wavelength, there are propagated surface modes (whispering gallery) with caustics positioned near the surface of the hole.

In comparison with a COF, the DCCOF has two more design parameters, which are refraction n_d and geometry d_d . For a set core refraction, the fundamental mode cut-off is determined mainly by core thickness d_r and numerical aperture NA_r , and much weaker by other parameters like hole diameter d_c , width of refractive depression in the cladding d_d and numerical aperture of the depression NA_d . The cut-off wavelength of fundamental mode increases with the core thickness and with the capillary hole diameter. Refractive characteristic of the fundamental mode of DCCOF as function of optical core thickness are analogous to the ones in COF with this difference that the values of derivatives dn_{eff}/dd_r and $dn_{eff}/d\lambda$, for $n_{eff} \approx n_p$ are bigger, which more precisely defines the very moment of the modal cut-off. The DCCOF has much bigger effective core area than the COF and W fiber at similar values of refractive and dispersion parameters.

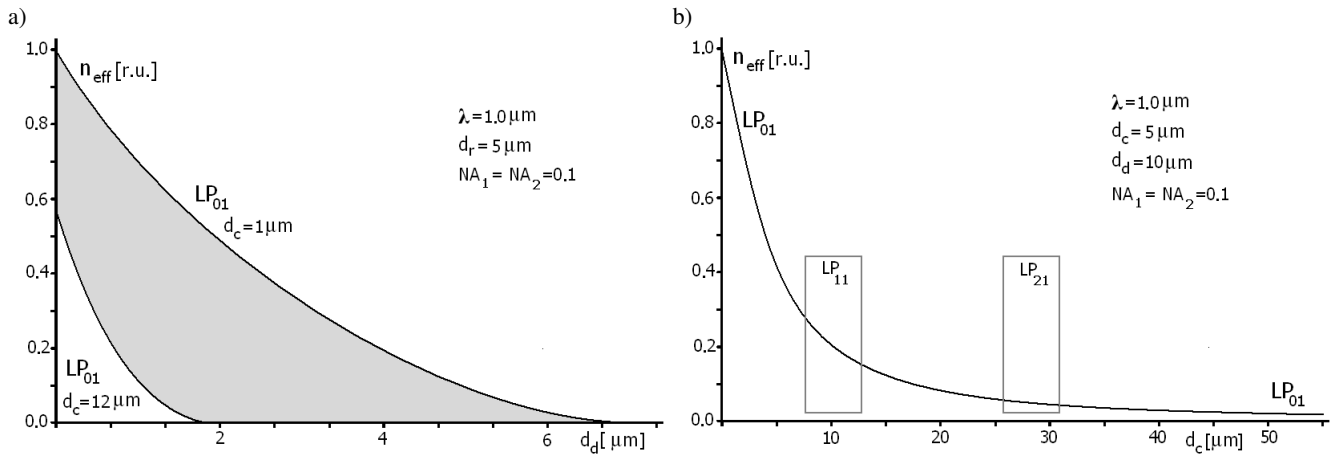


Fig. 3. Calculated relative effective refraction of fundamental mode in high silica DCCOF, (a) as a function of refractive depression thickness for different diameters of capillary hole, (b) as a function of capillary hole diameter, while the area left to the LP_{11} mode rectangle is purely singlemode

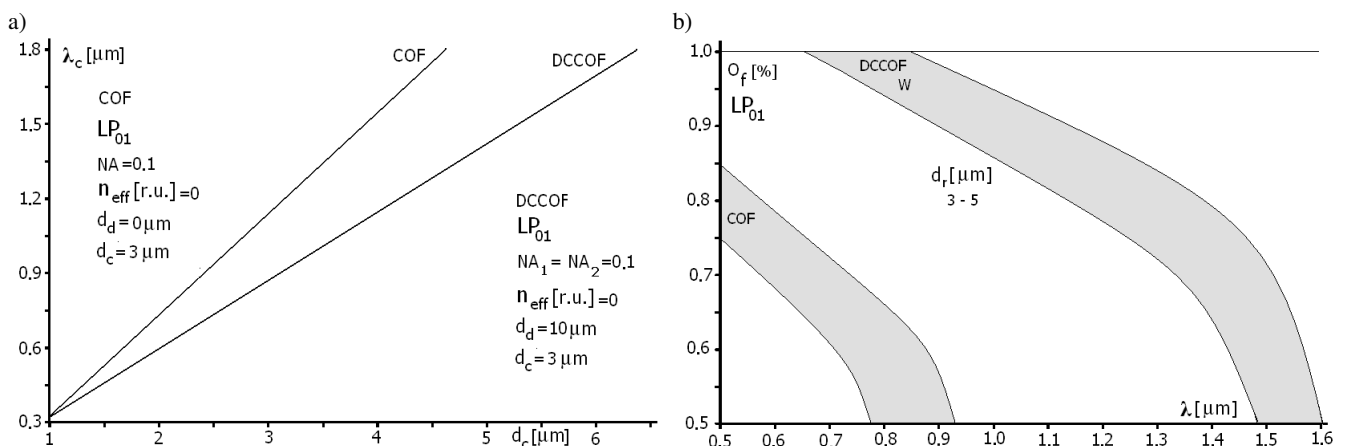


Fig. 4. (a) Calculated cut-off wavelength of fundamental mode for COF and DCCOF as a function of the hole diameter, (b) Changes in the overlap factor for the fundamental mode in COF, DCCOF and W fibers as a function of wavelength for different thickness of optical core d_r

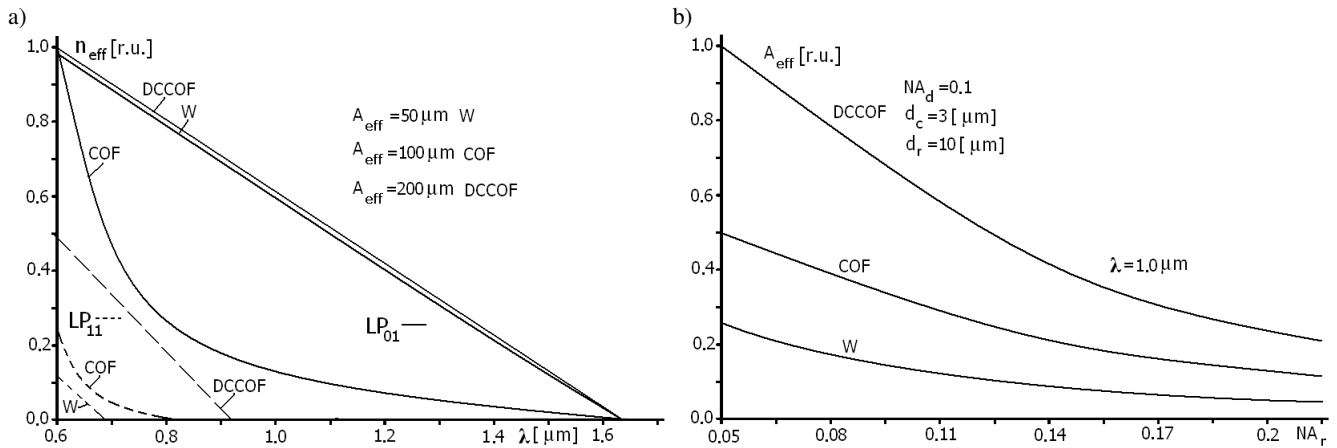


Fig. 5. (a) Comparison of calculated effective modal refraction for LP_{01} and LP_{11} for analogous fibers W, DCCOF and COF. (b) Comparison of calculated changes in the effective core area as a function of numerical aperture for analogous fibers W, DCCOF and COF

Figure 3a presents a singlemode area of DCCOF as a function of d_d and d_c parameters. For example, for $d_c = 5 \mu\text{m}$, the DCCOF is not guiding the fundamental mode, when the thickness of refractive depression in the cladding is bigger than $d_d > 3 \mu\text{m}$. The cladding refractive depression is an effective tool in designing the single mode area of DCCOF. Diameter of the hole also influences the fundamental mode cut-off. Large diameter of the hole (up to a certain value, keeping the fiber single mode) compensates large width of refractive depression in the cladding.

Figure 3b shows, on the background of the fundamental mode characteristic, the areas of cut-off changeability of the higher order modes which are difficult for separation. The areas were calculated for small, a few % changes in the DCCOF refraction and geometry. The fiber is unconditionally singlemode left to the LP_{11} rectangle. Then, the relative value of effective index is around 0.3, or not so much, i.e. the fundamental mode is weakly confined by the core and its field deeply penetrates other refractive layers of the fiber. For the wavelength $\lambda \approx 1 \mu\text{m}$ the fiber is singlemode for $d_c < 5 \mu\text{m}$ and for a considerable refractive depression in the cladding. Effective refraction of the fundamental mode grows when d_c is smaller, making the fiber more resistant to microbending losses. Smaller diameter of the hole causes stronger propagation of the fundamental mode in DCCOF, but also means smaller effective area of the core and lower efficiency of high power pumping. A compromise between the hole diameter and core thickness is a matter of fiber application.

DCCOF has a relatively broad possibility to shape the modal field distribution relative to its refractive and geometrical structure. In the active DCCOF (and in other active fibers) an important parameter is an overlap factor of the modal field with the doped area of the fiber, or the active core. The pumping area is different in various fibers: in DCCOF it is the whole area of the core and the hole, in double clad W and M fibers it is the inner cladding. The overlap factor in a COF, in the area close to fundamental mode cut-off, abruptly decreases, due to fast increase of the modal field diameter. The efficiency of COF laser is low. A different situation is in DCCOF, where

the optical field is more confined by the refractive depression in the cladding. Additionally, the field is less attenuated which is equivalent to more distinctive marking of the cut-off point, Fig. 4b.

Figure 5 shows a distinctive difference between the W, DCCOF and COF fibers relative to the effective area of the core. The smallest effective area is in the W fiber for equivalent refractive and geometrical parameters. Simultaneously, the W fiber has the broadest area where it is singlemode. The W and DCCOF are comparably resistant to microbending losses, while the COF is less resistive. Comparison of the analogous characteristics of COF and fibers from a similar family of refractive profiles gives necessary arguments for application of particular fibers in a variety of instrumental applications.

3. Fabrication

The basic studies on drawing of filaments were done in 60–70-ties, mainly for textile industry. These results were then adopted directly for fiberglass and optical fiber industry. Initially, a weakly perturbed fiber drawing model was assumed (strongly idealized). With the advent of the 90-ties, together with strong development of fiber specialization, especially the non-telecom fibers, the following additional factors were taken into account, during optical fiber drawing: heat transfer from laser beam, conical shape of the outflow meniscus and fiber coning, perturbations during the cooling phase, shaping of the initial glass drop, taking into account the inertial and gravitation forces, complex structure of the preform, viscosity level of glass expressed via the Rayleigh coefficient, heat transport mechanisms, strong mechanical instabilities [22]. Optical fibers and capillaries were subject to this analysis, together with deformation analysis of the capillary hole. Apart from many existing references concerning the manufacturing of capillary optical fibers, only few of them concern practical aspects of the drawing process, and in particular, obtaining a designed structure of glass-air surface. The most commonly given technological parameters of the drawing process are:

process temperature and influence of the surface tension on dimensions of the capillary hole. Also, only few papers compare the experimental results with numerical calculations.

A set of the Navier-Stokes and diffusion-convection equations transformed for glass capillary drawing geometry is as follows:

$$\begin{aligned} \rho(r_2^2 - r_1^2)(v_t + vv_z - g) \\ = [3\mu(r_2^2 - r_1^2)v_z + \xi(r_1 + r_2)]_z \\ (r_1^2)_t + (r_1^2v)_z = (r_2^2)_t + (r_2^2v)_z \\ = [p_0r_1^2r_2^2\xi r_1r_2(r_1 + r_2)]/\mu r_2^2 - r_1^2 \\ 0.5(r_2^2 - r_1^2)[\rho c_p(T_t + vT_z) - k(T_z)_z \\ - \sigma\varepsilon'(T_a^4 - T^4)] = r_2h(T_a - T) \end{aligned} \quad (3)$$

where: lower indexes mean a derivative of the function against the index argument, t – time, z – distance along capillary axis, r_1 and r_2 – internal and external dimension of capillary, v – velocity, ρ – density, g – gravity acceleration, μ – viscosity, p_0 – pressure difference between capillary and outside, ξ – surface tension, c_p – heat capacity, T – temperature, T_a – outside temperature, k – thermal conductance, σ – Stefan-Boltzman constant, ε' – material constant associated with emissivity, h – heat transfer coefficient. The equations stem from flow continuity laws, balance of momenta and energy. The capillary drawing geometry and boundary conditions for the Navier-Stokes equations are presented in Fig. 6. An initial assumption is that the capillary diameter is much smaller than the characteristic length of an outflow meniscus $r \ll L$. L is a length where the fiber dimensions are frozen.

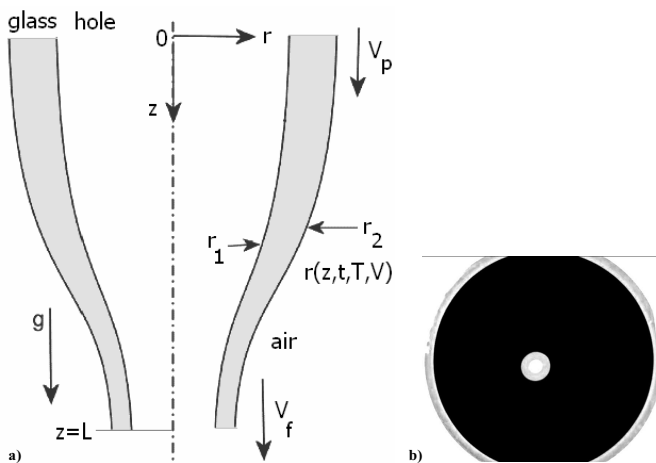


Fig. 6. (a) Geometrical set-up of COF drawing (not in proportion) for which the Navier-Stokes equations (3) were defined, and relevant defined parameters of the process: L – characteristic length of outflow meniscus, v_p – preform feeding rate, v_f – fiber pulling rate for outflow meniscus of capillary optical fiber, (b) photograph of a COF cross section $d_f = 125 \mu\text{m}$, $d_c = 7 \mu\text{m}$, $d_r = 4 \mu\text{m}$, $NA = 0.2$, $n_r = 1.6$

Figure 7 presents a few families of calculated normalized solutions of Navier-Stokes equations in a form of parametric curves. The parameters are technological values: velocity of preform feeding v_p , velocity of fiber drawing v_f , optical fiber diameter d_f , dimensional proportions in a capillary, pro-

cess temperatures T_{pi} . Analysis of the solutions to the Navier-Stokes equations leads to conclusions concerning technological conditions of manufacturing of optical fiber capillary.

The relative weight of major components influencing the COF drawing process: inertial, gravitational and surface tension is expressed by the following dimensionless factors: $LV_f\rho/\mu$, $gL^2\rho/\mu V_f$, $\xi L/\mu r_c V_f$, where L – characteristic length of high temperature meniscus (10–50 mm), V_f – characteristic velocity of fiber pulling (10–300 m/min), r_c – dimension of capillary hole (0.1–10 μm for single mode optical fiber, 30–500 μm for multimode optical fiber, 0.1–2 mm for discrete capillaries, 10–50 nm for nanocapillaries in photonic crystal fibers). Typical values of parameters, for high silica multi-component glasses are: $\rho = 2100\text{--}2600 \text{ kg/m}^3$ (2200 kg/m^3), $\mu = 10^4\text{--}10^5 \text{ Pas}$, $\xi = 0.3 \text{ N/m}$. Comparison of calculated values of the dimensionless factors reveals that the viscosity and gravity are always important, while inertia may be omitted. The surface tension and viscosity act in the opposite directions in the meniscus area. Geometrical proportions of the resulting fiber capillary depend on relative weight of these factors.

Overpressure in the capillary hole is characterized by the next dimensionless factor $Lp_0/V_f\mu$, where p_0 – pressure difference between capillary and vicinity (up to 10kPa). The effect of higher pressure in the capillary is visible for the technology, when the value of this factor is around 1. When there is no surface tension and differential pressure, the capillary hole does not collapse or expand, and the proportions are kept the same as in the preform.

Assuming even a small, but noticeable, surface tension (which condition is fulfilled at high process temperature), the viscosity dominates. Then, the capillary collapse processes depend on the rate of surface tension and viscosity ξ/μ . In these conditions, the hole closing is more sensitive to the velocity of preform feeding to oven, than to the fiber pulling rate. The viscosity is a strong function of temperature, thus the collapse process is too. The collapse is facilitated by low viscosity (high process temperature), slow preform feeding and long outflow meniscus (length of hot zone). Simplification of these complex considerations relies on the assumption that the whole meniscus is isothermal, and omitting of inertia, gravitation and pressure imbalance effects. If the inertia, gravitation and surface tension are skipped, in the isothermal case, then the technological process sensitivity to overpressure in the capillary is considerably increased. The above assumption is valid under the condition that the length of the hot zone is big, viscosity is low and preform feeding velocity is small.

When one takes into account the surface tension and overpressure in the capillary, the overpressure sensitivity of the process may be estimated. Assuming relatively not very big capillary hole, omitting the inertia and gravitation, for the isothermal case, the overpressure sensitivity may be expressed as follows: $S = L\xi/\mu R_1 V_p \log(V_f/V_p)$, where $R_1 = r_1(0)$ – internal radius of the preform, V_p – velocity of preform feeding. When $S \ll 1$, the overpressure is an efficient technological parameter tailoring geometrical proportions between

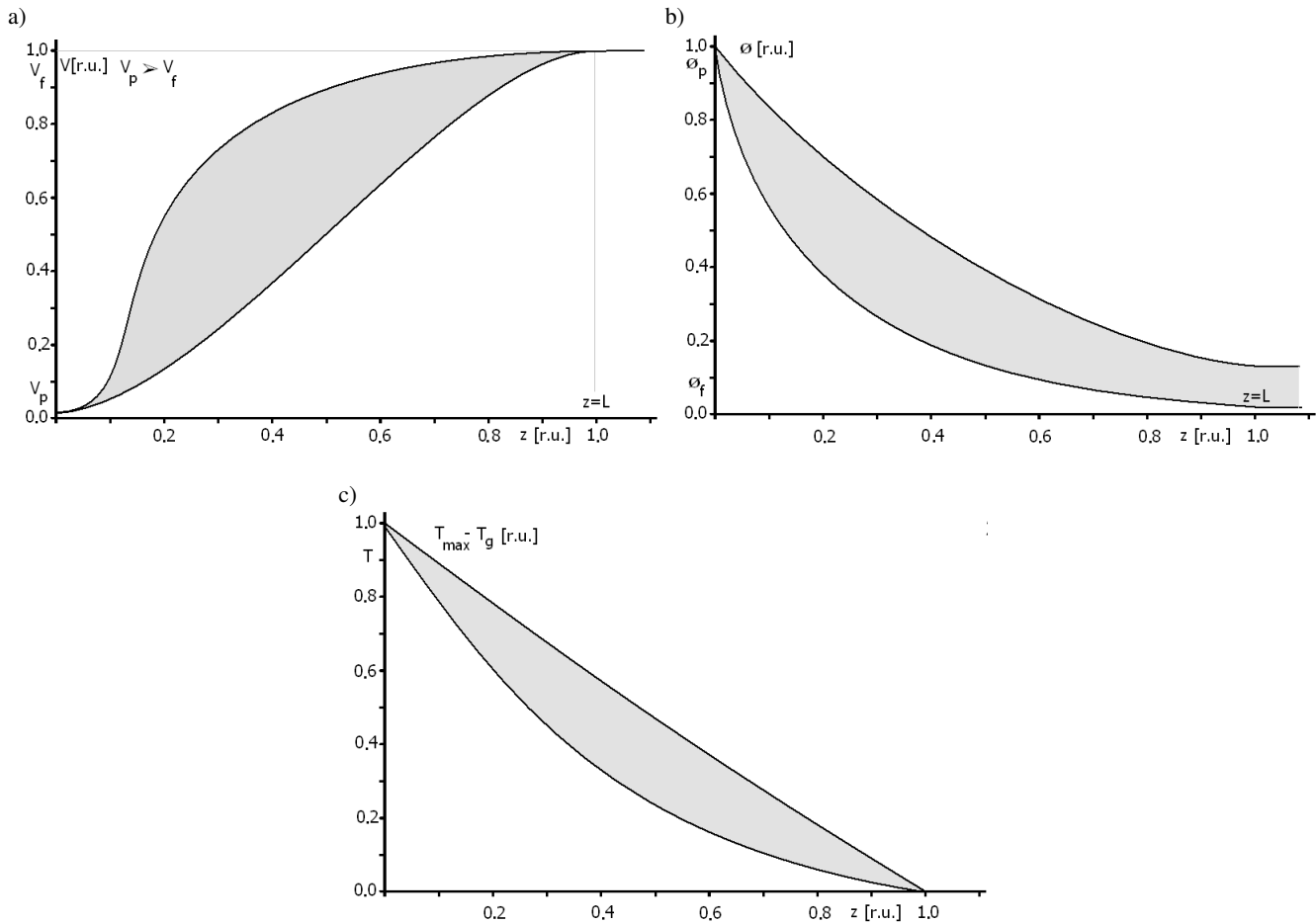


Fig. 7. Calculated normalized area for stationary solutions of Navier-Stokes equations formulated for hot fluid meniscus during fiber pulling. Particular solutions are discrete curves located within the area. $Z = 1$ is equivalent to characteristic length L of the meniscus. (a) Functional evolution of preform feeding velocity v_p [m/min] to fiber drawing velocity v_f [m/s], (b) Evolution of preform diameter d_p [cm] via local meniscus diameter d_m to fiber diameter d_f [μm], (c) Temperature distribution function along the meniscus

glass and air in the capillary. When $S \gg 1$, the technological set-up is very sensitive to the overpressure and fiber pulling is highly unstable, in these conditions. The S parameter is more sensitive to the preform feeding rate than to the fiber pulling rate. Because the hot zone length is constant for a particular process, and surface tension changes are small for high-silica glasses, thus the sensitivity depends only on the glass viscosity (i.e. on the pulling process temperature), on the initial dimension of hole in the preform, preform feeding rate, and ratio between preform feeding rate and fiber pulling rate V_f/V_p . The sensitivity increases for lower fiber pulling temperatures, smaller hole dimensions, lower preform feeding rates and lower values of velocity rate V_f/V_p . The calculated, exemplary results for the capillary hole diameter sensitivity to the technological process parameters (fiber pulling) are changing in the range of 0.1–3, for the following data: $r_1(0) = 1.5$ mm, $V_f = 190$ m/min, $V_p = 3$ mm/min, $T = 950^\circ\text{C}$. The conclusions are valid under the assumption that the technological process is isothermal in the meniscus zone. In reality, the inhomogeneous temperature distribution along the meniscus radius and axis influences the glass viscosity the most.

The main parameter deciding of the capillary collapse process is the ratio between glass surface tension and glass vis-

cosity. The surface tension in high-silica, multi-component glasses is weakly temperature dependent. The viscosity of pure silica and high-silica glasses is strongly temperature dependent. Thus, the pulling process temperature is a fundamental factor deciding of the capillary collapse. Similarly, the preform feeding rate decides more of collapse than the fiber pulling rate.

Relative dimensions of optical capillary depend on the rate of change of preform wall thickness, in the meniscus, along the fiber pulling axis. This rate depends fundamentally on the meniscus shape, i.e. on internal curvature, external curvature and external surface of the pulled capillary. In case of a full-glass optical fiber, the outflow meniscus depends on the most parameters of the technological process as: preform feeding rate, pulling temperature, preform and fiber dimensions, fiber pulling rate.

In practice, the pulling tower used for soft-glass high-silica optical capillaries is the same as for classical optical fibers. A photo of such a tower and a block diagram of the pulling process and associated measuring and control equipment are presented in Fig. 8. The parameters associated with capillary manufacturing can be divided to two groups: pulling process parameters, which are possible to be changed during

the process, and geometrical parameters, associated with the structure and dimensions of the preform and optical fiber. The most important process parameters are: fiber pulling temperature, preform feeding rate, overpressure in the capillary.

portions of capillary for different preforms were presented in Fig. 9. In several cases, with temperature increase (while keeping constant dimension of the capillary) the hole showed strong closing tendency.

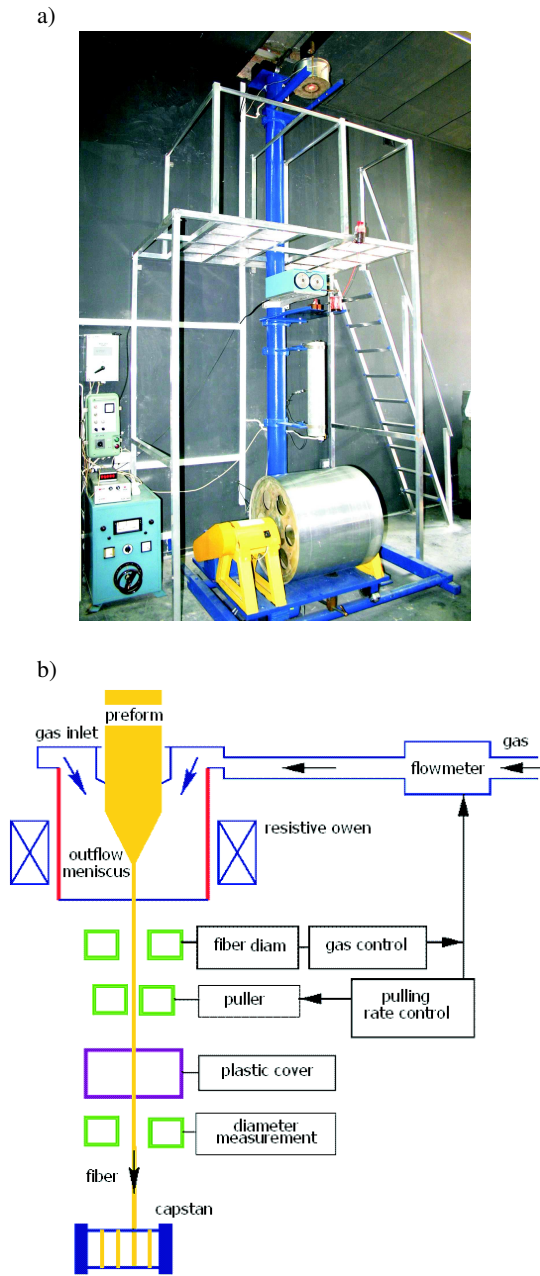


Fig. 8. Photograph of optical fiber pulling tower and block diagram of accompanying technological equipment

The capillary parameters, which can be changed during the process are: outside diameter (r_2) and inside diameter (r_1) which together determine the thickness of capillary wall. The ratio of both dimensions may be changed during the pulling through the influence on the collapse or expansion processes of the capillary hole. When the dimensional ratio r_2/r_1 in the fiber is greater than in the preform, a partial collapse occurred during the pulling process. In the opposite case, the hole was expanding. Measurements of the changes in dimensional pro-

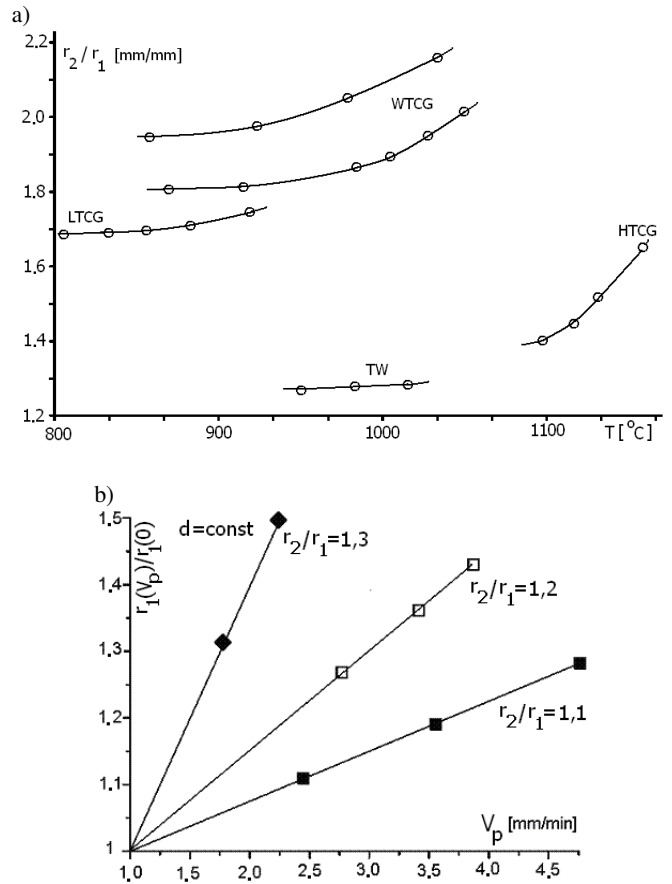


Fig. 9. (a) Change of the ratio of dimensions – external r_2 to internal r_1 in a capillary optical fiber, as a function of pulling temperature for five different preforms of different high-quality optical soft-glasses, WTCG-wide temperature compound glass preform, LTCG-low temperature, HTCG-high temperature, TW-thin wall preform. The measured function images the collapse (or expansion) processes of the capillary hole, (b) Relative increase in optical fiber capillary hole $r_1(V_p)/r_1(0)$ diameter with increase in preform feeding rate V_p , for three different preforms of the same high-quality optical soft-glass and of various r_2/r_1 ratio and for $d = r_2 - r_1 = \text{const}$

A basic task during the capillary manufacturing is control of constant value of the wall thickness $d = r_2 - r_1$. These dimensions are related by $r_2/r_1 = r_2/(r_2 + 2d) = (r_1 + 2d)/r_1$. The collapse avoidance relies on the maximization of viscosity forces during the pulling process, via lowering of the temperature. Possibility to control the wall thickness allows for manufacturing of dimensional series of capillaries out of a single preform.

The process of capillary collapse takes place only in the upper part of the outflow meniscus, where the temperature is the highest. The lower part of meniscus is a place, where the dimension proportions of capillary are frozen, despite the fact that the outer diameter of intermediate fiber still undergoes strong reduction. The collapse is improbable in the lower part of the meniscus, despite the increasing forces of surface

tension (which are the main cause of collapse) with decreasing diameter of the capillary. Axial force, induced by the fiber pulling process, causes the increase in the viscosity considerably faster with lowering of the capillary dimension (through decreasing of temperature). The influence of surface tension is meaningful only for bigger capillary diameters (created in bigger outflow meniscus, of bigger heat capacity). The result of relevant measurements and calculations were presented in Fig. 9a and 9b.

Changes of the dimensional ratio r_2/r_1 were measured along a capillary, during the pulling process, for a few pre-forms. Table 1 gathers the measurement results for two pre-forms $r_2 \cdot d : 8 \times 1.1$ mm and 34×1.5 mm, where $d_p = r_2(0) - r_1(0)$ preform thickness and $d_f = r_2(L) - r_1(L)$ capillary thickness, where L-characteristic length of fiber pulling, Fig. 6a. Standard deviation of measurement results for the capillary is bigger than for the preform. The increase of standard deviation of dimensions in the pulled capillary fiber is caused by other factors than the stability of dimensional proportions in the preform. These are supposedly technological factors associated with the capillary collapse. The conclusion is that the wall thickness should be strictly controlled during the capillary pulling process.

Table 1

Measurement comparison of changes in dimensional proportions in preform and capillary

preform r_1/d [mm]	preform		capillary	
	average value r_2/r_1	standard deviation [%]	average value r_2/r_1	standard deviation [%]
8×1.1	1.075	0.01	2.3	0.3
34×1.5	1.0075	0.02	1.15	1.1

The longitudinal stability of capillary diameter is as important parameter as a constant value of dimensional proportions r_2/r_1 . The longitudinal stability of outer diameter of capillary fiber were measured. The exemplary results, measured for preform 34×1.5 , $T = 1050^\circ\text{C}$, $V_f = 11$ m/min, for optical fiber of nominal dimensions $125 \mu\text{m}$ were $\pm 0.25 \mu\text{m}$. In order to obtain a capillary optical fiber of good quality, the changes in external dimensions have to be minimized. The sources of changes in external dimensions of fiber are: changes in preform dimensions, changing parameters of technological process, mechanical vibrations (microphonics) of the pulling tower, stability of furnace temperature, parameters of laminar, insulating gas flow in the furnace, overpressure in the capillary. According to the rule of mass flow continuity, the change of preform of exemplary dimension of 34 mm and height/length perturbation of 1mm will be extended on the length of a few hundred mm, for a fiber of $125 \mu\text{m}$ in diameter. The change in preform diameter influences the shape of outflow meniscus and gas flow distribution adjacent to the meniscus. Through this subtle change, it influences the dynamics of the pulling process. Characteristic frequency of dimension changes in fiber is considerably higher than in the preform.

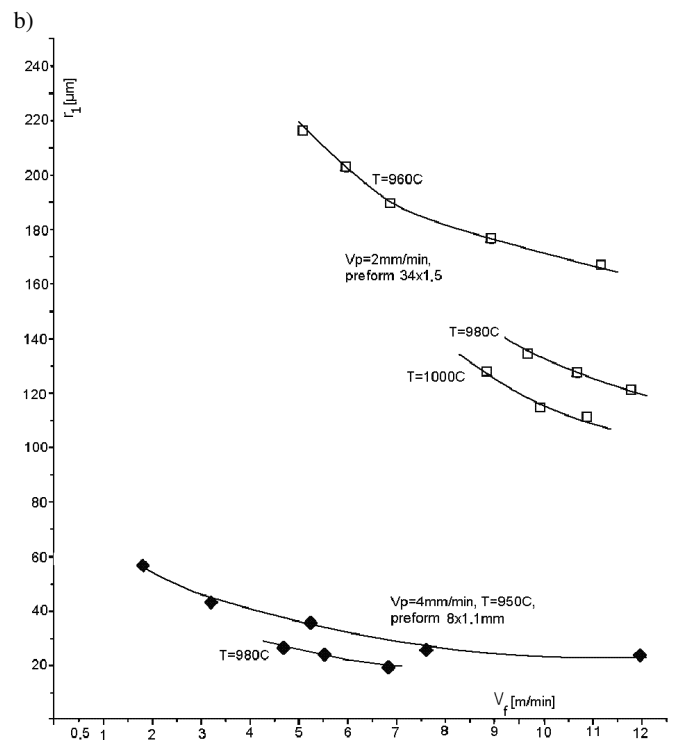
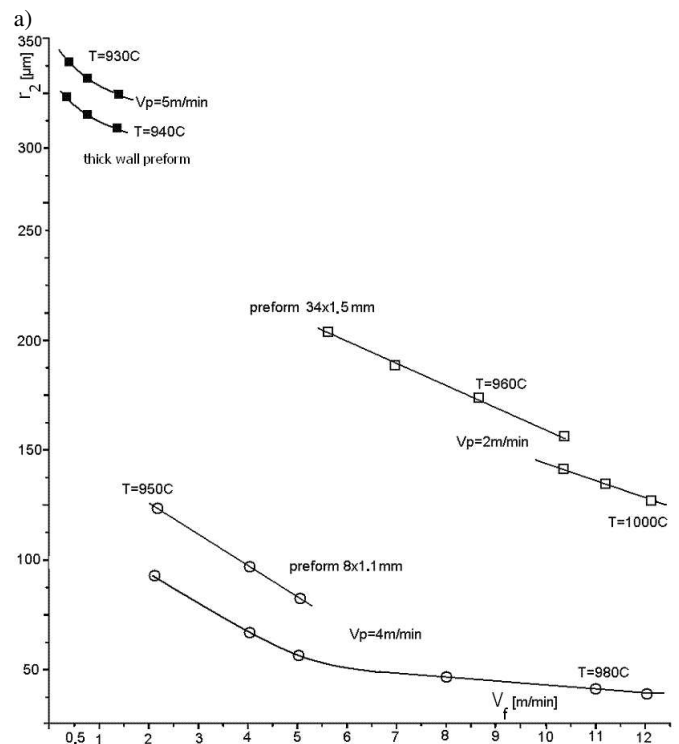


Fig. 10. Experimental results (measurement points) and numerical solutions of the N-S equations (continuous lines) for the external r_2 and internal r_1 diameter of COF, as function of fiber pulling rate V_f for various preforms, pulling temperatures T_p and preform feeding rates V_p

A change in the feeding velocity of preform changes the oven temperature in the vicinity of meniscus. The faster the preform is fed, the shortest time stays in the hot zone. Distribution of viscosity changes in the meniscus, is influencing

the collapse mechanisms. Preform feeding rate (aside of the temperature) is one of the parameters for control of geometrical proportions of the optical fiber capillary. It is, however, not a very efficient parameter, because of big time constant of this method of control (too big control loop latency). Dimension of the capillary hole depends strongly on the preform feeding rate, thus this rate has to be stable. Fig. 9b presents measured, relative dependencies of internal capillary diameter on preform feeding rate. When the feeding is very slow, the capillary is subject to collapse. In these conditions, small changes in the preform feeding rate cause big changes in the capillary diameter.

Figure 10 presents the measurement results and comparison with the numerical calculations for both capillary diameters – internal and external. The data used for calculations were: length of hot zone in the furnace, pulling parameters, physical and chemical data of the glasses used for optical capillary manufacturing. The higher furnace temperatures, lower preform feeding rates, and bigger rates of optical fiber pulling, all together lead to smaller dimensions of the capillary holes. For bigger rates of the preform feeding, final dimensions of

the capillary are more sensitive to the pulling rate, than for smaller rates of the preform feeding. For typically used pulling process parameters, the capillary collapse is quite weak. This phenomenon is a strong function of the preform feeding rate.

In order to obtain a capillary optical fiber which images the geometrical proportions of the preform, one has to obey the following rules for technological parameters of the pulling process: hot zone of the furnace should be the shortest (shortening of the outflow meniscus), process temperature should be the lowest acceptable, preform feeding rate to the furnace should be the highest acceptable, the preform and the capillary optical fiber should have relatively big holes dimensions.

4. Characterization

The pulled capillary optical fibers were characterized optically and mechanically using standard measuring equipment for classical fibers with modified signal coupling techniques. The details of measurement set-ups are presented elsewhere [1]. Table 2 summarizes some of the parameters of available COFs.

Table 2
Parameters of manufactured COF and DCCOF

Parameter, measure	Kind, value
kind of glasses	high silica, multicomponent: lime-calcium, lime-barium, lime-lead, borosilicates
refraction	around 1.5 for high silica, typically 1.55–1.75 for compound, special higher refraction available on demand
fabrication	complex crucible, extrusion, pulling from preform, hybrid-combined
geometrical dimensions [μm]	a series of standardized types for internal capillary dimensions with 150 μm of fiber outside dimension or special dimensions on demand, especially of smaller diameters
external diameter – fiber [μm]	standard dimensions in the range 30–350, special dimensions out of this range available on demand
internal diameter	standard dimensions 5–200, small dimensions capillary 1–5, special dimensions outside these ranges available – capillary hole [μm] on demand
stability of transverse dimensions	standard dimensional stability better than 3 for the length sample of COF, special dimensional stability better than 1% of COF [%]
average ellipticity [%]	Standard ellipticity lower than 1 per sample length
protective jacketing	Standard polyamide, hard, double-layered, on demand soft silicone,
internal thin film layer	Non-protected or protected capillary hole after fiber fabrication, capillary surface conditioning
Conditioning materials	Water, hydrogen, oxygen, inert gases, polymers, polyolefins, Teflon, tetra,
range of optical transparency [nm]	Typically 400–2000, depending on COF material
Average level of transparency	90%/5 m in the visible range
refractive index profile	Step-index, multi-step index
Internal numerical aperture	Typically 0.05–0.3, bigger on demand
External numerical aperture	0.05–0.3, bigger on demand
Mechanical strength [GPa]	0.3–1.5
Weibull parameter	3–7
Average breaking radius of curvature	Around 3–5 mm for 50 μm , around 15 mm for 200 μm
Length of provided COF samples for research and applications	A series of standardized dimensions, typically 20–40 cm, 1 m, 5 m, longer length samples on demand
Time of COF sample delivery	2 weeks for a fiber from a series of standardized types, 2 months for a fiber out of the series of standardized types
Other fabricated specialty optical fibers	ring-core, multi-ring core, elliptical core, of complex refractive index profile like M and W, noncircular core, special material, sensitized and desensitized

5. Applications

The availability of COFs has recently awakened locally the interest in optical capillary based assemblies, modules and MOEMS. A number of fabricated and characterized COF samples, mainly in a series of standardized types, were made available by the technological centers for application partners. The fibers were primarily used for manufacturing of sensors and microoptic functional devices. Prior to that the access to more specialized and/or nonstandard COF and DCCOF fibers was confined.

5.1. Microfluidics. A controlled flow of minute amounts of fluids (liquids and gases alike) is a key to the construction of laboratory on chip microsystems (LOC) [23]. Optically enhanced microfluidics embraces such devices, mainly planar but also capillary, as transmission channels, semi-insulated cavities, reactors, traps, windows, reactants inlets and outlets, optical inputs and outputs, optical or piezo pumps, splitters, couplers, etc. Optically enhanced microfluidics uses such methods and processes like wave and matter transport, pumping, mixing, heating or cooling, optical excitation, optical or electro-optical measuring like pH-metry, spectroscopy, etc.

A series of experiments was performed on construction of a COF based amplitude microoptic modules [24] with a mobile microdroplet for the following applications in microfluidics, micro systems and optical microsensors: position sensors via shift of a microdroplet in a capillary and CCD read-out, frequency measurement of a microbeam resonance with the center of gravity changes introduced by microdroplet shift, pressure difference sensor between microcells in a microsystem, optically controlled transport of matter in microsystems, microdroplet microlens properties modulation, two phase – gas and liquid – flow measurement, etc. A side advantage of microfluidics systems is the possibility to make optical measurements of manipulated fluid microsamples.

The measurement set up of a COF system with mobile microdroplet was presented in Fig. 11. The microdroplet acts as an optical microlens and as a movable mass. The basic optical characteristics of this system were measured like signal transmission and sensitivity to external reactions like thermal and mechanical. Figure 11c presents two photos of the cross-section of applied COF in the micromodule. The fiber is filled with a series of spaced microdroplets. The photo shows presence of the ballistic modes for a short span of COF and core modes for a longer span. This effect of switching between the ballistic and core modes is obtained also as a result of beam defocusing by the microlens and is effective irrespective to the fiber length. The microlens is a strong filter for ballistic modes. The measured characteristics show the performance of the opto-mechanical-microsystem. The curve in Fig. 11d shows changes in optical power transmission as a function of microdroplet positioning in the capillary. For different liquid, or for conditioned capillary surface, the lens may be convex. Under the external influence the lens may change from convex to concave and vice versa. The positioning may be done thermally, electrically or mechanically (pressure). The character-

istic in Fig. 11e shows changes in optical power transmission as a function of microlens refraction. The refraction may be changed thermally or electrically, thus, the system is a kind of MOEMS. The applied optical fiber capillaries are acting simultaneously in this experiment as classical capillaries. This set up enables wide spectrum of optical measurements, including longitudinal or transverse ones, and an active energetic interaction of optical wave with microscopic amount of transmitted material medium. Adding optics via COF technology to the microfluidics opens new areas in the MOEMS technology.

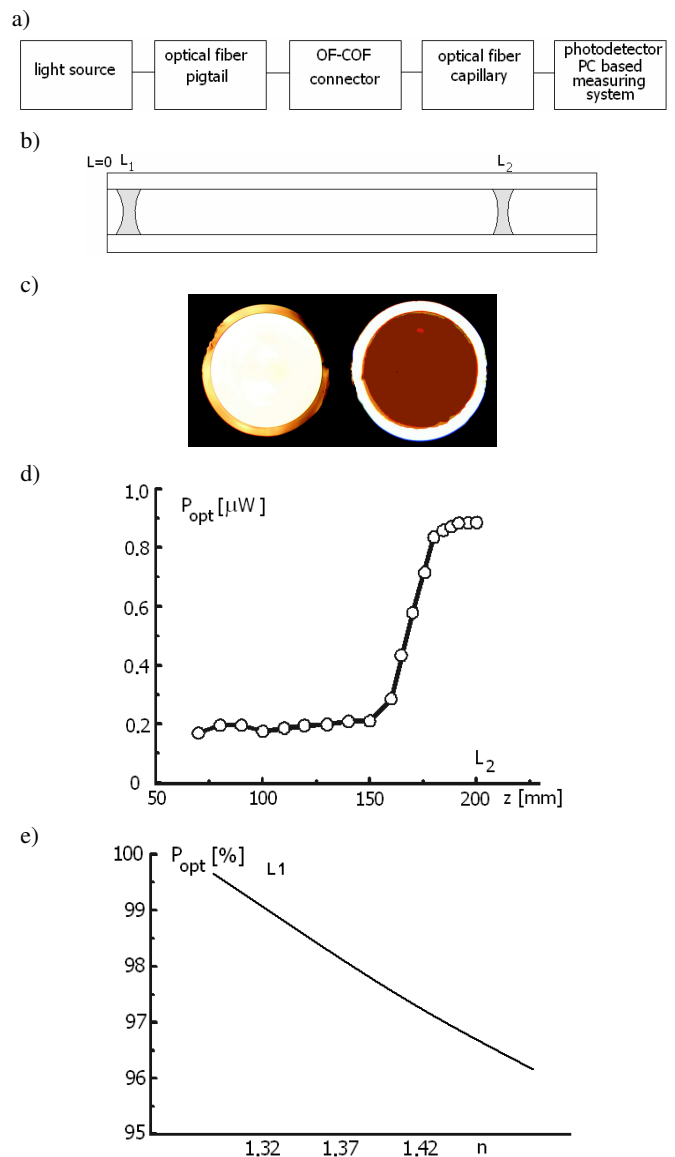


Fig. 11. (a) Measurement set-up and functional diagram of the microfluidic device, (b) ray tracing in capillary with microdroplets, (c) capillary fiber end faces with ballistic and core modes, (d) measured characteristics of microoptic module with COF filled with liquid microdroplet lens, (e) changes in optical power transmission as a function of microlens refraction. Fiber data: multimode, $d_f = 300 \mu\text{m}$, $d_c = 260 \mu\text{m}$, two fiber sample lengths $l_1 = 50 \text{ mm}$, $l_2 = 300 \text{ mm}$. Microdroplet lens data: concave, volume 300 nl, length on fiber axis $L_1 = 0.9 \text{ mm}$, $L_2 = 1 \div 200 \text{ mm}$. Measurements done for $\lambda = 670 \text{ nm}$ (after Ref. 19)

5.2. Micro-refractometry. Optical refractometers or spectrometers based on capillary optical fibers confine the measured media to the capillary core and increase the sample interaction lengths, thus enhancing the intensity of spectroscopic image. Capillary made of glass, even low-index one is capable of transmitting light by total internal reflection only for high-index liquids. Capillary made of amorphous fluo-

ropolymer (Teflon), having a refractive index of 1,29 is capable of supporting optical wave transmission virtually for any liquid, including aqueous, alcohol and light aromatic hydrocarbons solutions. Thus, some of the COF refractometers for low index liquids have to be fabricated of low-loss transparent Teflon, instead of glass.

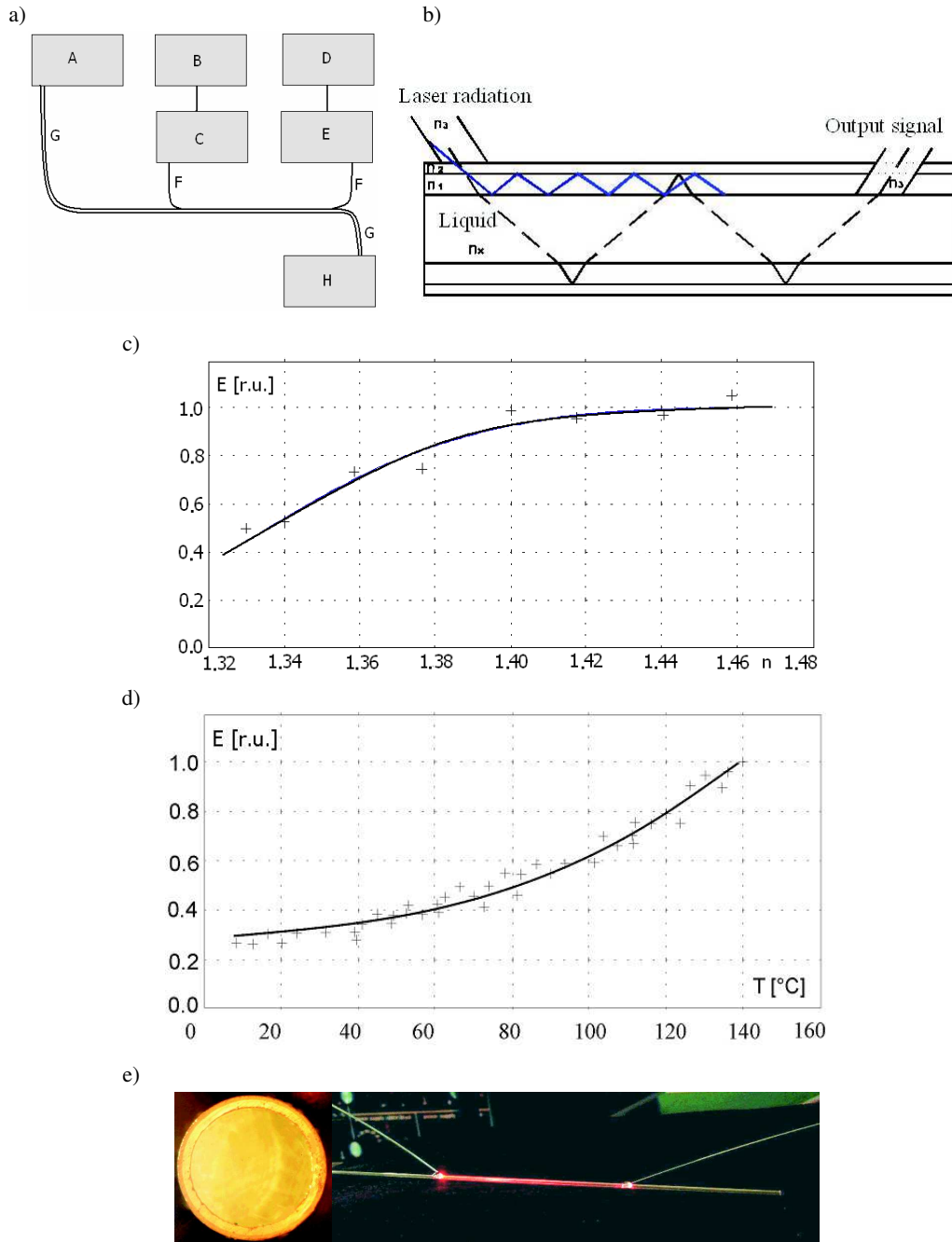


Fig. 12. (a) Measuring set-up for calibration of a COF microrefractometer, A – container with normalized glucose solution or alternatively with a measured liquid, B – stabilized power supply, C – He-Ne laser, D – optical power meter, E – detector, F – multimode optical fiber for power delivery, G – capillary optical fiber, H – sink for flowing liquid; (b) Construction of the optical coupling between COF and a classical transmitting and receiving fibers; (c) Measured calibration characteristic of the COF based microrefractometer, electrical output E as a function of liquid refraction. COF is filled with glucose solution; (d) Measurement characteristic of a COF refractometer used for in-flow oil thermometry; (e) a photo of a COF set-up used for the construction of the microrefractometer in longitudinal and transverse views after Ref. 20. E [r.u.] is a signal on the detector in relative units. Fiber data: outside diameter 1300 μm , outside diameter of optical core 1100 μm , capillary hole diameter 800 μm , $n_1 = 1.524$ $n_2 = 1.510$ after Refs. 20, 21. $T = 20^\circ\text{C}$

A number of amplitude and phase COF based microoptic modules were constructed for refractometry, colorimetry, opacimetry and optical thermometry. Some of them also base on the microfluidics solutions. There were measured refractions of the muster solutions of glucose for the COF sensor calibration. Configuration of the measuring set-up, construction of the COF-classical fiber coupler, calibration curve and refractometer photo were presented in Fig. 12. Figure 12e shows a close up view of the capillary cross section and fiber refractometer transmitting HeNe laser radiation coupled from and back to a multimode telecom grade fiber from above. The telecom fibers are connected to the light source and to the detector.

The calibration curve of COF microrefractometer, Fig. 12c is based on the dependence of molar refraction of two component solution: $R_{12} = x_1R_1 + x_2R_2 = [(n^2 - 1)(x_1M_1 + x_2M_2)]/\rho_{12}(n^2 + 2)$. The refraction is $n_{12} = \sqrt{3R_{12}\rho_{12}/(M_{12} - R_{12}\rho_{12}) + 1}$, where n_{12} is the refraction of the mixture, ρ_{12} is density, R_{12} is molar reactivity, M_{12} molar mass of the mixture. The accuracy or refraction measurements is $\pm 10^{-3}$. The constructed COF microrefractometer is used for determination of unknown refraction of fluids. It is used as a continuous flow sensor in chemical processes.

5.3. Flow micro-thermometry. The same principle, as presented in Fig. 12a was used for the construction of a capillary flow microthermometer [21] The capillary was positioned on a Peltier cell and a heater. As above, its predicted applications is in MOEMS as well as in electrically insulated systems. The temperature of oils was measured via the known changes of their refractive index $n(T)$ [25], Fig. 12d. The increase in temperature causes a different decrease of refraction specific to particular kind of oil. In-flow oil recognition sensor is based on this principle. The relevant dependence, binding the refractive index n with material density ρ and temperature T , is the Lorentz-Lorenz formula: $(n^2 - 1)/(n^2 + 2)\rho = 4\pi f(1 - F)/3$, where f is average polarizability, F is molecular correction factor expressed as expansion series of f . A two phase flow was observed in some oils above 150°C, which was a sign of oil degassing.

5.4. Gas sensors. Capillary optical fiber gas sensors use immobilized indicators lining with a thin layer the surface of a capillary hole [23]. The immobilizing agents depend on the active substance of the indicator. They are for example: ammonium (or other chemically binding substance) as a chemical bond and cellulose matrix or hybrid xerogels as mechanical fixture. The xerogels are composed of alkyl and perfluoroalkyl ORMOSILs (organically modified silicates). The xerogels display good adhesion to the glass surface and are prone to doping with a range of different indicators. The indicators depend on the gas to be detected. In case of CO₂, the indicators are HPTS, PTS, TOA, TOAOH.

The mechanism of gas detection is based either on pH changes or on fluorescence intensity modulation of the indi-

cator. The gas dissolves in the sensing layer, which is bonded directly to the internal glass fiber surface either changing the system pH or quenching the fluorescence. The sensing chamber of long length but small volume provides short reaction time, usually of the order of tens of s . The quality of the sensor depends on the technology of the dyes which are immobilized in polymer and on polymer membranes. The measuring range of sensor is determined by particular application. In the case of methane these are safety regulations or for CO₂ this is the range of water dissolution for this gas, i.e 1–20 hPa. The accuracy of measurement in the latter case should be better than 1 hPa. The calibration of COF gas sensor is done by exchanging the measured gas atmosphere with the inert gas like helium or nitrogen and measuring the reaction time or presence of the process hysteresis. Usually the reaction time from inert gas to the measured medium is very fast but in the reverse it is an order of magnitude longer. This is associated with washing out of the measuring substance and saturation processes in the indicator. The experiments with usage of cellulose matrix and hybrid xerogels doped with HPTS in COF gas sensors show the increased response, sensitivity, measuring range and speed of these devices.

5.5. Micro-optics. Several microoptic and micro-opto-mechanical components based on the fabricated COFs were developed at our and partner laboratories. These are basic devices necessary for laboratory work with advanced fiber optic systems and MOEMS. They embrace: permanent and reusable connectors between classical fibers and COFs, COF T and Y splitters with capillary hole continuity, alignment microdevices for COFs and classical fibers, COF tapers, single-mode and multimode COF patch cords, standardized dimensionally precision optical tubing, COF connectors to planar microsystems with buried optical waveguides and matter channels, etc.

The dimensional compatibility decides frequently of the direct and easy application of COF in existing microsystems. It concerns mainly fitting with classical optical fibers. COFs of standardized external dimensions equal to 125 μm and 150 μm were used together with classical optical fibers for construction of micro Fabry-Perot resonators, for modal filters, etc. Such fibers are also used for building the Y and T splitters. COFs of standardized internal dimensions equal to 125 $\mu\text{m} + 1 \mu\text{m}$ and 150 $\mu\text{m} + 1 \mu\text{m}$ were used as the precise mechanical tubing with optical alignment insight and for other related purposes. COF dimensions used for the microoptics are gathered in Table 3.

Other parameter, apart from the dimensions, deciding of practical applications of COF is maintaining the continuity of the capillary in combined branched microsystems supporting the transmission of wave and matter. One of the basic solution to this is to use standardized open channel connectors, adapted from the classical chemical capillary techniques and modified to optical purposes to enable low-loss optical connectivity.

Table 3
Dimensional specifications of COFs for fabricated microoptic applications

application field / dimensions [μm]	optical aligning components	micromechanical coupling	microbeams for MOEMS	micromechanical switches	chemical sensors	optical sensors
hole diameter [μm]	125–127, 150–152	50	50, 100	125	200	200, 300
outside diam. [μm]	150, 200	125	100, 125, 150	150, 200	300	300, 500

6. Conclusions

Capillary optical fibers are used more and more frequently in practical applications like sensors but still not as frequently as classical fibers and classical capillaries. It stems from very strong economic domination of classical chemical capillary technologies with the global market of hundreds M\$ and from the conservative approach of chemical industries. The simplest way to broad applications in this area is to replace classical capillaries with their optically enhanced analogies. They immediately provide active optical interaction with the transported chemical medium. They require, however, a supplement of optical infrastructure like transmitters, receivers and analyzers attached to classical capillary paths.

Together with the development of COF technique a new terminology was introduced. The COFs are also known as optical fibers with a macro-hole, as differentiated of the ones with micro-holes. Both types of fibers are named together as hollow or holey – the latter name is reserved for photonic fibers. Optical fibers with an internal discrete hole are of the following kinds: the core as a hole, a hole close to the core, the core around a hole and the core suspended in air or the core in the hole. A beginning to these technologies stems from chemical capillaries turned to liquid filled core optical fibers.

Potential applications of COFs are broad and stem from the following factors and effects: transmission of large optical power in air core, large influence of the hole on optical core, filling the core with a measured medium, large interaction length between the medium filling the core and the evanescent or guided wave, guidance of various waves like surface WGM, modulation of surface tension in liquids filling the capillary, usage of different guidance mechanisms – refractive and diffractive-interference.

Recent developments in COF applications are associated with optical wave transmission using Von Neumann-Wigner mechanism and coherent transmission of singlemode deBroglie wave inside a dark light beam. The latter is associated with strictly ordered transmission of single cold atoms. COF nanometer tapers are used as tips for optical version of an atomic force microscope (AFM). The investigated surface is probed with single helium atoms emanating from the COF tip. Other atoms are deposited in single quantities on a surface (active inversed lithography) in an ordered way by such a probe.

The COFs have different properties, and thus application perspectives, as classical optical fibers. The fundamental feature is close proximity between an external interaction and the

optical guided field. This proximity makes the COF based device very sensitive. The best example of this kind of sensibility is an integrated COF spectrometer with evanescent wave, with the measured medium filling the hole. Such a spectrometer makes a part of a microsystem.

The research on COF application use frequently the filaments of standard dimensions like 125 μm and 150 μm . It stems from the availability of measuring equipment for the telecom fiber geometry standards. The most frequently used internal diameter of capillary is a few μm for singlemode and a few tens μm for multimode COFs. The following practical devices were constructed of COFs and side-hole optical fibers: integrated temperature and strain sensors, polarizers, elasto-optic components, chemical sensors, amplitude and phase sensors, spectrometers, optodes and components for microsystems.

The availability of COF samples, as a result of realization of the program PBZ Optoelectronic Modules, supplements the existing offer of tailored optical fibers delivered previously for the research purposes as a result of realization of the program PPPW Photonics Engineering. The availability of COFs has clearly activated the interest in research on such micro-system technologies as MOEMS and LOC. The basic parameters of COFs for the users, relevant to the applications under development, turned out to be: kind of glass, refraction, geometry – external dimensions and internal proportions between hole and optical core. The COF material determines the sensitization method to a particular external reaction the fiber is subject to. The COF refraction determines the kind of refractive environment the fiber is used in. The COF geometrical proportions determines fiber usage as an amplitude or phase sensor.

Acknowledgements. The work on capillary optical fibers was supported by the Research Program on “Optoelectronic Components and Modules for Applications in Medicine, Industry, Environment Protection and Military Technology”, PBZ-MIN-009/T11/2003 (2004–2007).

The author acknowledges cooperation with prof. J. Dorosz and his co-workers of Białystok University of Technology on fabrication, characterization and application of capillary optical fibers.

The author acknowledges cooperation with prof. W. Woliński of Warsaw University of Technology, chair of the Research Program on Photonics Engineering (1995–2001) and selected part of Research Program on Optoelectronic Components and Modules (2004–2007).

REFERENCES

- [1] R. Romaniuk and J. Dorosz, *Design and Fabrication of Capillary Optical Fibers*, Technical Report, Grant PBZ-MIN-009/T11/2003 (2003–2007), Warsaw University of Technology, 2007, (in Polish).
- [2] A.B. Sotsky and L.I. Sotskaya, “Modes of capillary optical fibers”, *Optics Communications* 230 (1–3), 67–79 (2003).
- [3] M.A. Olshanii, Yu.B. Ovchinnikov, and V.S. Letokhov, “Laser guiding of atoms in a hollow optical fiber”, *Opt. Commun* 98, 77–80 (1993).
- [4] J.F. Giuliani, *Optical Fiber Sensor for Methane Gas*, US Patent 4708941, 1987.
- [5] R. Altcorn, I. Koev, R.P. VanDuyne, and M. Litorja, “Low-loss liquid-core optical fiber for low-refractive-index liquids: fabrication, characterization, and application in Raman spectroscopy”, *Applied Optics* 36 (34), 8992–8998 (1997).
- [6] J. Bravo, I.R. Matias, I.D. Villar, J.M. Corres, and F.J. Arregui, “Nanofilms on hollow core fiber-based structures: an optical study”, *J. Lightwave Technol.* 24 (5), 2100–2105 (2006).
- [7] K. Matsumura, Y. Matsumura, and J.A. Harrington, “Evaluation of gold, silver and dielectric coated hollow glass waveguides”, *Opt. Eng.* 35, 3418–3421 (1996).
- [8] V. Neves and A.S.C. Fernandes, “Modal characteristics of A-type and V-type dielectric profile fibres”, *Microwave and Optics Technology Letters* 16(3), 164–169 (1998).
- [9] R. Romaniuk and J. Dorosz, “Technology of soft-glass optical fiber capillaries”, *Proc. SPIE* 6347, 634711–634718 (2006).
- [10] E.A.J. Marcatili and R.A. Schmetzer, “Hollow metallic and dielectric waveguides for long distance optical transmission”, *Bell Syst. Tech. J.* 43, 1783 (1964).
- [11] D.H. Bilderback, “Review of capillary x-ray optics from the 2nd International Capillary Optics Meeting”, *X-Ray Spectrometry* 32, 195–207 (2003).
- [12] P. Glas, M. Nauman, A. Schirmacher, and T. Pertsch, “Neodymium-doped hollow optical fiber laser for applications in laser-guided atoms”, *Proc. CLEO* 60, 428–429 (1998).
- [13] P. Polynkin, A. Polynkin, N. Peyghambarian, and M. Mansuripur, “Evanescent field-based optical fiber sensing device for measuring the refractive index of liquids in microfluidic channels”, *Opt. Lett.* 30, 1273–1275 (2005).
- [14] P.J.A. Sazio, A. Amezcua-Correa, C.E. Finlayson, J.R. Hayes, T.J. Scheidemantel, N.F. Baril, B.R. Jackson, D.J. Won, F. Zhang, E.R. Margine, V. Gopalan, V.H. Crespi, and J.V. Badding, “Microstructured optical fibers as high-pressure microfluidic reactors”, *Science* 311, 1583–1586 (2006).
- [15] J. Mrazek, V. Matejec, M. Hayer, J. Skokankova, I. Kasik, D. Berkova, and F. Kostka, “Capillary optical fibers modified by xerogel layers for chemical detection”, *Proc. SPIE* 6180, 618013.1–6 (2006).
- [16] Department of Optical Fiber Technology, Maria Curie-Skłodowska University, <http://www.umcs.lublin.pl/jednostki.php?id=323>.
- [17] Department of Optical Radiation, Białystok University of Technology, <http://vela.pb.bialystok.pl/~kpo/>.
- [18] PBZ-MIN-009/T11/2003, “Optoelectronic components and modules for applications in medicine, industry, environment protection and military technology”, Ministry of Science and Informatization, http://kbn.icm.edu.pl/finauki98/PBZ/lista_projektow_20031020.html, 2003.
- [19] M. Borecki, M.J. Korwin-Pawłowski, M. Bełowska, “Light transmission characteristics of silica capillaries”, *Proc. SPIE* 6347, 634741–634747 (2006).
- [20] P. Miluski and D. Dorosz, “Measurement of refractive index using capillary waveguide”, *Proc. SPIE* 6347, 634742–634746 (2006).
- [21] P. Miluski, “The temperature sensor based on capillary waveguide”, *Proc. SPIE* 6937, 693755–683759 (2007).
- [22] M. Gregory Forest and Hong Zhou, “Unsteady analyses of thermal glass fibre drawing process”, *Europ. J. Applied Mathematics* 12, 479–496 (2001).
- [23] A. Dybko, Warsaw Univ. Technology, Faculty of Chemistry, Department of Chemical Sensors, private communications.
- [24] M. Borecki, Warsaw Univ. Technology, Institute of Micro and Optoelectronics, Department of Microsystems Technology, private communications.
- [25] S.A. Khodier, “Refractive index of standard oils as a function of wavelength and temperature”, *Optics and Laser Technology* 34, 125–128 (2002).